GEOCHEMISTRY OF EARLY SIDERITE CEMENTS FROM THE EOCENE SUCCESSION OF WHITECLIFF BAY, HAMPSHIRE BASIN, U.K.

JENNIFER HUGGETT[1]*, PAUL DENNIS[2], AND ANDY GALE[3]
[1] Department of Geology, Imperial College of Science, Technology and Medicine, Prince Consort Rd. London SW7 2BP, U.K.
e-mail: JMHuggett@aol.com
[2] School of Environmental Sciences, University of East Anglia, Norwich NO4 7TJ, U.K.
[3] School of Earth Sciences, University of Greenwich, Grenville Building, Central Parade, Chatham Maritime, Chatham, Kent, ME4 4AW, U.K and Department of Palaeontology, Natural History Museum, Cromwell Road, SW7 5BD, U.K.

ABSTRACT: **Siderite cements in the Eocene of Whitecliff Bay (Hampshire Basin, U.K.) occur in a range of depositional facies and morphological associations. Most siderites are associated with *in situ* glaucony or occur beneath conspicuous lithological breaks. These associations illustrate the importance of slow deposition for early diagenetic carbonate precipitation. Siderite in the Eocene sediments of Whitecliff Bay is impure and in many cases comprises zoned crystals, with an overall decrease in substitution of Ca, Mg, and Mn for Fe from crystal core to rim. Trends in Ca, Mg, and Mn from early to later siderite vary between samples, with no evident environmental control.**

Siderite concretions without calcite cement occur only beneath lithological breaks where meteoric water may have been introduced. Precipitation temperatures have been calculated from siderite $\delta^{18}O$ data and are based on the assumption that precipitation occurred from seawater. These temperatures are reasonable for typical microbial siderite precipitated in marine sediment but are slightly low for marine siderite where there may have been meteoric overprinting. If the precipitation temperature for siderite cements is assumed (from $\delta^{18}O$ data for time-equivalent biogenic carbonate) rather than the composition of the precipitating fluid, the calculated isotopic composition of the precipitating fluid is generally compatible with the inferred marginal marine depositional environments.

INTRODUCTION

The geochemistry of early siderite cements has been previously described from both marine (Machemer and Hutcheon 1988; Matsumoto 1989; Mozley and Hoernle 1990; Mozley and Carothers 1992) and nonmarine to brackish sediments (Pearson 1974; Pye et al. 1990; Gibson et al. 1994; Al-Agha et al. 1995). In the Eocene clastic sediments of the Harwich Formation, the London Clay Formation, and the overlying Bracklesham Group at Whitecliff Bay, Isle of Wight (Fig. 1), siderite-cemented beds and concretions occur in both shallow marine and estuarine facies in a variety of sequence stratigraphic settings, thus providing the opportunity to compare the geochemistry of siderite formed across environmental gradients. The Eocene succession at Whitecliff Bay is one of the most complete in southern England. In addition to cliff exposures transecting the almost vertically tilted succession, rare exposures after storms have stripped the wave-cut platform of sand provide the opportunity to collect unweathered material. The London Clay Formation consists of a series of upward-coarsening units (divisions A–E of King 1981), with an overall upward increase in grain size (Fig. 2). The sedimentology of the Bracklesham Group has been studied in detail by Plint (1983, 1988). Sedimentation occurred in a shallow marine to estuarine setting throughout the depositional history. Lithological details are provided in Huggett and Gale (1997, 1998).

METHODS

Concretions were collected from ten horizons (two or three per horizon) from beach exposures at Whitecliff Bay, Isle of Wight. Two siderite-cemented beds and a mudrock with $< 5\%$ siderite cement were also sampled. Sample locations are marked in Figures 2 and 3 and are quoted in the text as height above the base of the Harwich Formation. All samples were examined in back-scattered electron (BSE) imaging mode using a Hitachi S2500 scanning electron microscope equipped with an Oxford Instruments 860 analyzer. Quantitative energy-dispersive X-ray (EDS) analyses were obtained from polished blocks using a 2 μA beam current at 15 kV accelerating voltage. EDS data were recalculated as cation mole fractions to facilitate comparisons among samples. All mineral percentages are visual estimates derived from BSE images. $\delta^{13}C$ and $\delta^{18}O$ isotope analyses were carried out at the University of East Anglia, School of Environmental Sciences. Samples were crushed and ground to a powder prior to analysis. In all cases the cement zoning is too fine scale to separate individual zones by microdrilling. Reaction conditions were 100°C for 36 hours with 102% phosphoric acid for pure siderite samples. For samples with both siderite and calcite, the selective acid extraction method of Al-Aasm et al. (1990) was used. The samples are first reacted at 25°C to extract CO_2 from the calcite fraction, then at 100°C to obtain CO_2 from the siderite. Fractionation factors of 1.01025 (CO_2 from calcite) and 1.00881 (CO_2 from siderite) were used to calculate the carbonate $\delta^{18}O$ from the measured CO_2 compositions (Rosenbaum and Sheppard 1986). Replicate measurements of the internal laboratory standard (UEACMST—Carrara Marble) give total analytical precisions of $\pm$ 0.07‰ for both carbon and oxygen measurements. All values are quoted with respect to VPDB (Vienna Peedee Belemnite).

RESULTS

Siderite Facies Associations

Type 1.—Type 1 siderite occurs only as cement in the cross-bedded, transgressive shallow marine glauconitic sandstone (10–15% glaucony) at the base of the Harwich Formation (Fig. 2). Sandstones of the Harwich Formation contain abundant serpulid tubes and glaucony pellets. The base of the London Clay Formation is burrowed into the underlying Harwich Formation, with glaucony concentrated in the burrows.

Type 2a.—Type 2a siderite occurs as concretions ellipsoidal in vertical sections, circular in the plane of bedding, and 0.05–0.2 m in maximum diameter. This siderite type is restricted to the highest part of the London Clay Formation and in the Wittering Formation of the overlying Bracklesham Group (Fig. 3). All these concretions occur in very fine to fine glauconitic sandstone, except for those from the basal bed of the Wittering Formation (Fig. 3; 150.1 m; sample WIT7), which occur as an erosional conglomerate lag. The elemental data for WIT7 siderite are identical to those of LCF6 from the uppermost London Clay Formation, which suggests that WIT7 was derived by reworking of the LCF6 concretion horizon.

Type 2a concretions are concentrated in beds beneath surfaces of nondeposition and erosion, specifically where lagoonal facies (intertidal laminated sandstone and mudstone, plus infill of an abandoned tidal creek) overlie glauconitic or muddy sandstone deposited in open marine shelf

* Present address: School of Earth Sciences, University of Greenwich, Grenville Building, Central Parade, Chatham Maritime, Chatham, Kent ME4 4AW, U.K.

JOURNAL OF SEDIMENTARY RESEARCH, VOL. 70, NO. 5, SEPTEMBER, 2000, P. 1107–1117
 1073-130X/00/070-1107/$03.00

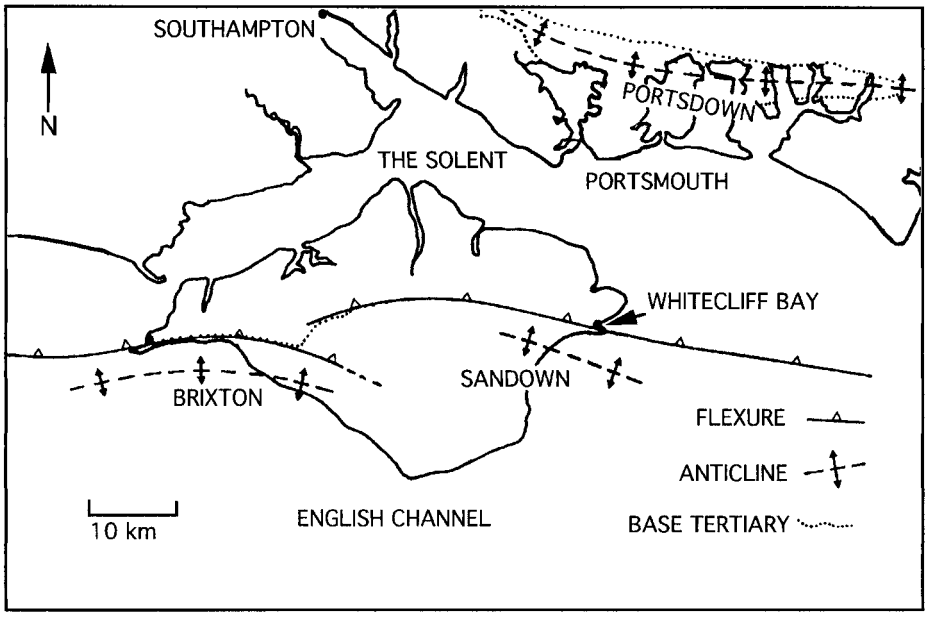

FIG. 1.—Map of the Hampshire basin showing the location of Whitecliff Bay.

environments (Fig. 3). Seven such levels were found during the present study between the upper part of the London Clay Formation and the Bracklesham Group. Plint (1988; his fig. 4) interpreted lagoonal mudstones and sandstones of the Bracklesham Group in Whitecliff Bay as having accumulated behind a transgressive barrier bar and representing the first stage of transgression. Subsequently, the wave-dominated barrier migrated landward, cutting a marine ravinement surface on which a lag of pebbles accumulated. A succession of open marine shelf facies accumulated on this surface until a fall in sea level created the next lowstand erosion surface (sequence boundary), beneath which siderite concretions developed. Concretions occur beneath three types of nondepositional or erosional surfaces:

1. Siderite concretions in the upper part of the London Clay Formation and in the Wittering Formation occur 1–2 m beneath conspicuous lithological breaks (151 m and 187.7 m; E1 and E2 of Plint 1983) between shelfal glauconitic sandstones below and lagoonal laminated sediments above. These are interpreted as composite sequence boundaries/transgressive surfaces (Huggett and Gale 1997, 1998). Two layers of Type 2a concretions are present 0.5–2 m beneath each of these erosion surfaces: LCF5 and LCF6 below E1 (Fig. 3) and WIT13 and WIT15 below E2. A sparse conglomerate of reworked siderite concretions (WIT7) of 0.05–0.1 m maximum diameter is present immediately above E1.

2. Erosional surfaces at 144.2 m and 172 m channel downward by as much as 2 m into muddy, glauconitic shelf sandstones and are filled with laminated sandstone and mudstone of intertidal facies. We interpret these as abandoned tidal-creek channels and tentatively identify them as sequence boundaries (SB? in Figure 3) in addition to the two described above. Type 2a siderite concretions are found 0.1–1.5 m beneath both of these surfaces (LCF4 is from 143 m, which is below the surface at 144.2 m, and WIT9 is from immediately below the surface at 172 m). LCF4 concretions contain well preserved and articulated crustaceans (J. Quayle, personal communication), suggesting that cementation was extremely early.

3. The upper part of the Wittering Formation is composed of laminated intertidal and lagoonal sandstones, siltstones, and claystones and a conspicuous, deeply rooted (roots extend down 4–5 m) freshwater lignite bed at 198.2 m (the ''Whitecliff Bay Bed''). Siderite concretions (WIT 33) occur 4 m beneath the lignite (194.2 m) in a fine-grained sandstone.

Type 2b.—Four siderite-cemented beds a few centimeters thick occur in the upper part of Division B2 of the London Clay Formation (at 55.2–58 m). The beds were deposited in a fully marine environment (indicated by the fauna) and consist of partially laminated, very fine silty sandstone to clayey siltstone.

Type 2c.—Ellipsoidal concretions of both siderite and ferroan calcite with a 10–30 cm maximum diameter occur at various levels in the London Clay Formation (35 m, WH18B; 64, WH19; see Fig. 2). These concretions occur in bioturbated silty claystone and clayey siltstone with $<$ 1% glaucony. The siderite forms rims around silt-size grains and are overgrown by calcite (Fig. 4F).

Type 3.—Siderite as discrete rhombs and in association with alteration of mica are a minor ($\leq$ 1%) component throughout the unweathered sediments, regardless of facies association, mineralogy, or grain size. A slight enrichment (3% visual estimate) of Type 3 siderite occurs in fully marine sediments at 40 m (WH8, Fig. 2), where glauconitic sandy mudrock (5% glaucony) is overlain by silty mudrock. The contact between the two lithologies is not erosional, but the burrowed, glauconitic surface indicates a pause in deposition.

Petrography and Geochemistry

Type 1.—The cemented beds are 20% siderite, with quartz, K feldspar, glaucony (10–15%), clay, abundant serpulid tubes, and framboidal pyrite (1–3%). The siderite is an intergranular cement, consisting mostly of unzoned lozenges (Fig. 4A). The siderite appears to have overgrown framboidal pyrite. The mean mole fractions of the siderite are 0.79 Fe, 0.02 Mn, 0.1 Ca, and 0.09 Mg (Table 1). The carbonate has a higher proportion of isotopically light oxygen than any other siderite type ($-$5.5‰ VPDB); the carbon is relatively heavy ($-$5.65‰ VPDB) (Fig. 5A–C).

Type 2a.—The concretions are 50–80% siderite, the clastic component is composed of quartz, K-feldspar, glaucony (1–10%), clay, and framboidal pyrite ($<$ 1%). Siderite crystals are 2–5 μm in maximum length, subhedral, and chemically zoned in all concretions examined except WIT7, which has a microcrystalline cement without compositional zoning resolvable by BSE microscopy (Fig. 4). Zoned cement crystals typically vary from mid gray at the core to dark gray (least substitution for Fe), to mid gray to light gray (highest Mn substitution) at the rim (Fig. 4C–D). For simplicity, in the following discussion we refer to overall trends using compositions of crystal rims and cores only. In general, substitution of Fe by Ca and Mg is lower than in Type 1, and Mn substitution is greater (Table 1, Fig. 5). Despite similarity in BSE images of LCF5 (Fig. 4C) and WIT 15 (Fig. 4D)

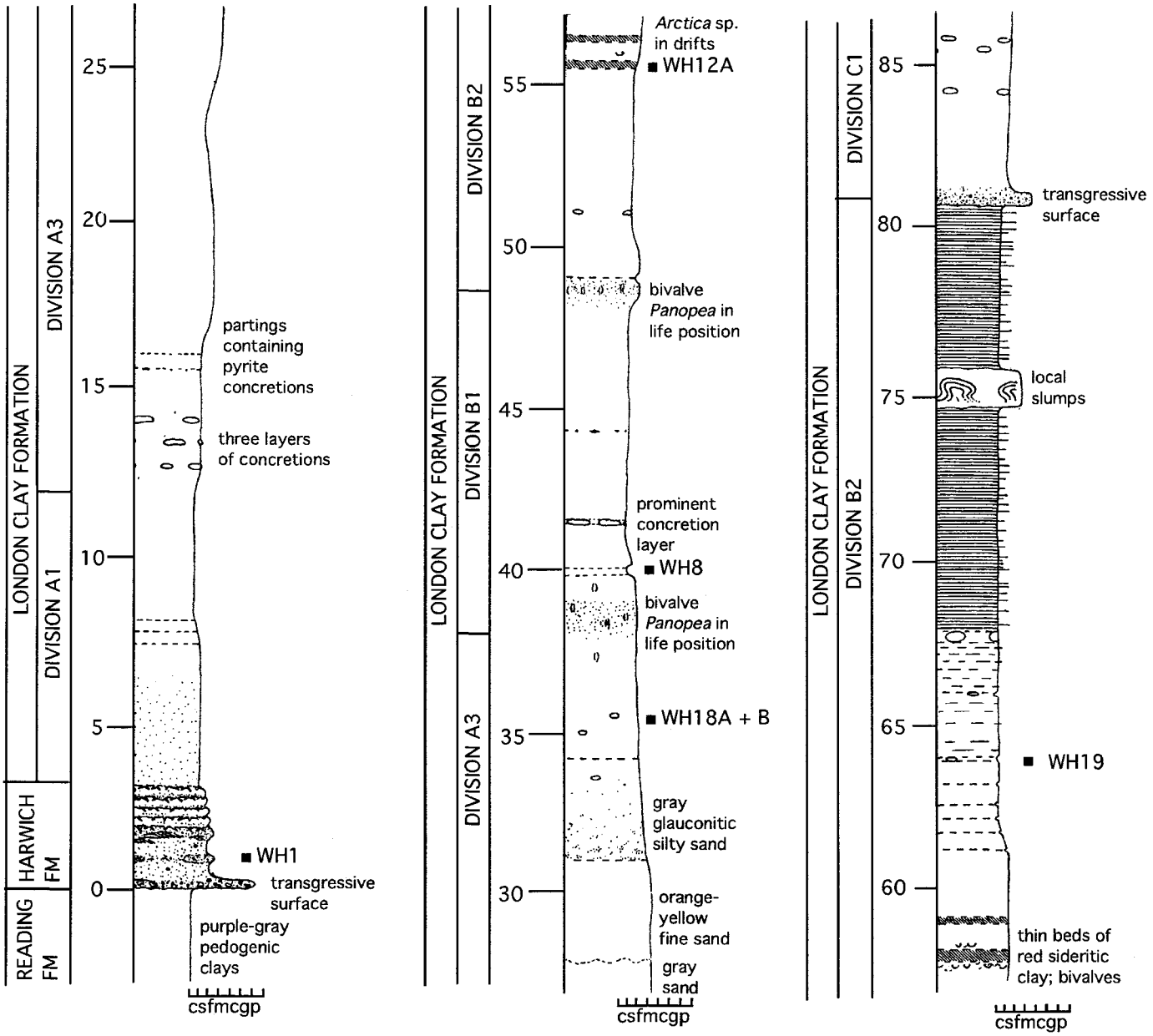

FIG. 2.—The Harwich Formation and the lower part of the London Clay Formation on the foreshore at Whitecliff Bay, with sample locations marked. Grain-size scales are indicated at the base of each lithological column.

the trends for Ca and Mg mole fractions are slightly different. In LCF5 mean mole fractions of substituted ions are 0.08 Ca, 0.07 Mg, and 0.02 Mn for the cores, and 0.03 Ca, 0.02 Mg, and 0.04 Mn for the rims. In WIT15 mean mole fractions are 0.04 Ca, 0.02 Mg, and 0.1 Mn for the earlier siderite, and 0.04 Ca, 0.03 Mg, and 0.07 Mn for the later siderite. Concretion WIT13 has the highest Mn concentration (mean mole fraction 0.12); WIT15 and WIT33 are also high, with mean Mn mole fractions of 0.06 to 0.10 (Table 1). Concretions with zoned cements show a decrease in total substitution of Fe from crystal core to margin. Whole-rock siderite stable isotopes (presumed to be an average of rim and core cement) for Type 2a siderite range from −13.97‰ to 3.99‰ VPDB for $\delta^{13}C$ and −2.1‰ to 0.81‰ VPDB for $\delta^{18}O$ (Table 2). The $\delta^{18}O$ values are heavier than for the other siderite types (Fig. 5D–F). Ca and Mg concentrations increase, and Fe and Mn concentration decrease, with decreasing bulk $\delta^{18}O$ (Fig. 5D–F). However, the seemingly similarly zoned LCF5 and WIT15 (mostly early Fe ''poor'' siderite, Fig. 4C–D) have quite different carbon isotope values.

Type 2b.—Siderite constitutes 10–40% of these beds. The clastic component is dominated by quartz and clay, with minor K-feldspar and mica. Framboidal pyrite (2%) and rare euhedral pyrite occur as inclusions in the siderite cement; glaucony is absent. The siderite is microcrystalline, subequant, and chemically zoned with crystal rims very slightly enriched in Fe and Mn (Fig. 4E, Table 1). Whole-rock stable-isotope values (presumed to be an average of rim and core cement) are −13.3 and −12.93‰ VPDB for $\delta^{13}C$ and −3.13 and −2.62‰ VPDB for $\delta^{18}O$ (Table 2). These data are similar to those for LCF5 (type 2a) despite the differences in elemental chemistry and appearance (Fig. 4).

Type 2c.—These predominantly ferroan calcite concretions have 5–10%

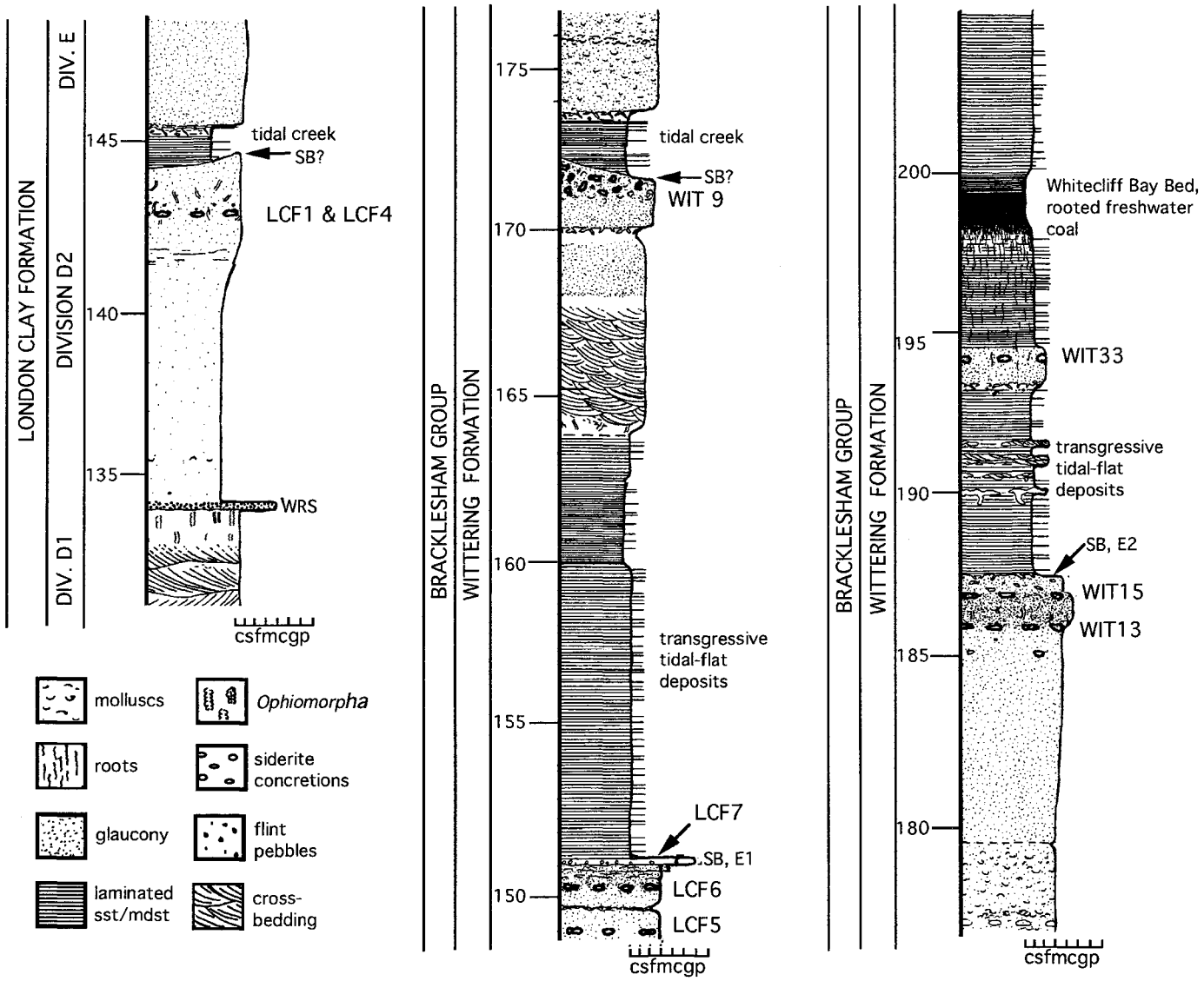

FIG. 3.—The upper part of the London Clay Formation and the lower part of the Wittering Formation on the foreshore at Whitecliff Bay, with sample locations marked. WRS = wave ravinement surface, SB = sequence boundary. E1 and E2 are erosion surfaces. Grain-size scales are indicated at the base of each lithological column.

grain-rimming siderite (Fig. 4F). The ferroan calcite has overgrown both the siderite and rare pyrite crystals resting on the siderite. The mineralogy of the host sediment is dominated by quartz and clay, with minor K-feldspar, mica, < 1% glaucony, and 1–2% framboidal pyrite. Mean mole fractions for substituted cations in WH18A and WH18B are 0.1 and 0.08 for Ca, 0.1 and 0.13 for Mg, and 0.1 for Mn. Whole-rock siderite stable isotopes range from −19.55 to −8.15‰ VPDB for $\delta^{13}C$ and −5.22 to −2.13‰ VPDB for $\delta^{18}O$ values (Table 2).

Type 3.—This siderite association consists of mudrock with ≤ 3% siderite rhombs. The clastic component is dominated by quartz and clay, with minor K feldspar, mica, glaucony (≤ 5%) and framboidal pyrite (1–2%). This siderite has the lowest mean Mn mole fraction (< 0.01) and highest mean Mg mole fraction (0.14) of any Whitecliff Bay siderite analyzed (Table 1). The mole fractions for Ca and Fe are 0.06 and 0.81, respectively. Given the low concentration of siderite in WH8 and hence the small amount of material that could be extracted, the stable-isotope analyses may not be

→

FIG. 4.—Back-scattered electron micrographs of siderite cements. **A)** Lozenge-shaped siderite (S) cement in clay matrix of the Harwich Formation sandstone (WH1). Some crystals have hollow cores; possibly these were high-Mg calcite seeds for the siderite. Scale bar = 25 μm. **B)** Cryptocrystalline nonzoned siderite from concretion WIT7. Scale bar = 12 μm. **C)** Subequant siderite from concretion LCF5. The cement has three chemical zones with > Fe and Mn, < Ca and Mg in the light rim compared with the mid-gray core; the intervening dark zone is too narrow to analyze without contamination. Scale bar = 30 μm. **D)** Subequant siderite from concretion WIT15. The cement has three chemical zones with > Fe and Mn, < Ca and Mg in the light rim compared with the mid-gray core; the intervening dark zone is too narrow to analyze without contamination. Scale bar = 30 μm. **E)** Subequant siderite from cement bed WH12A. The cement has two chemical zones with > Fe and Mn, < Ca and Mg in the light rim compared with the dark core. Scale bar = 30 μm. **F)** Grain-rimming microcrystalline siderite cement (arrow), with later ferroan calcite (F) cementing and replacing clay-rich matrix. Scale bar = 30 μm.

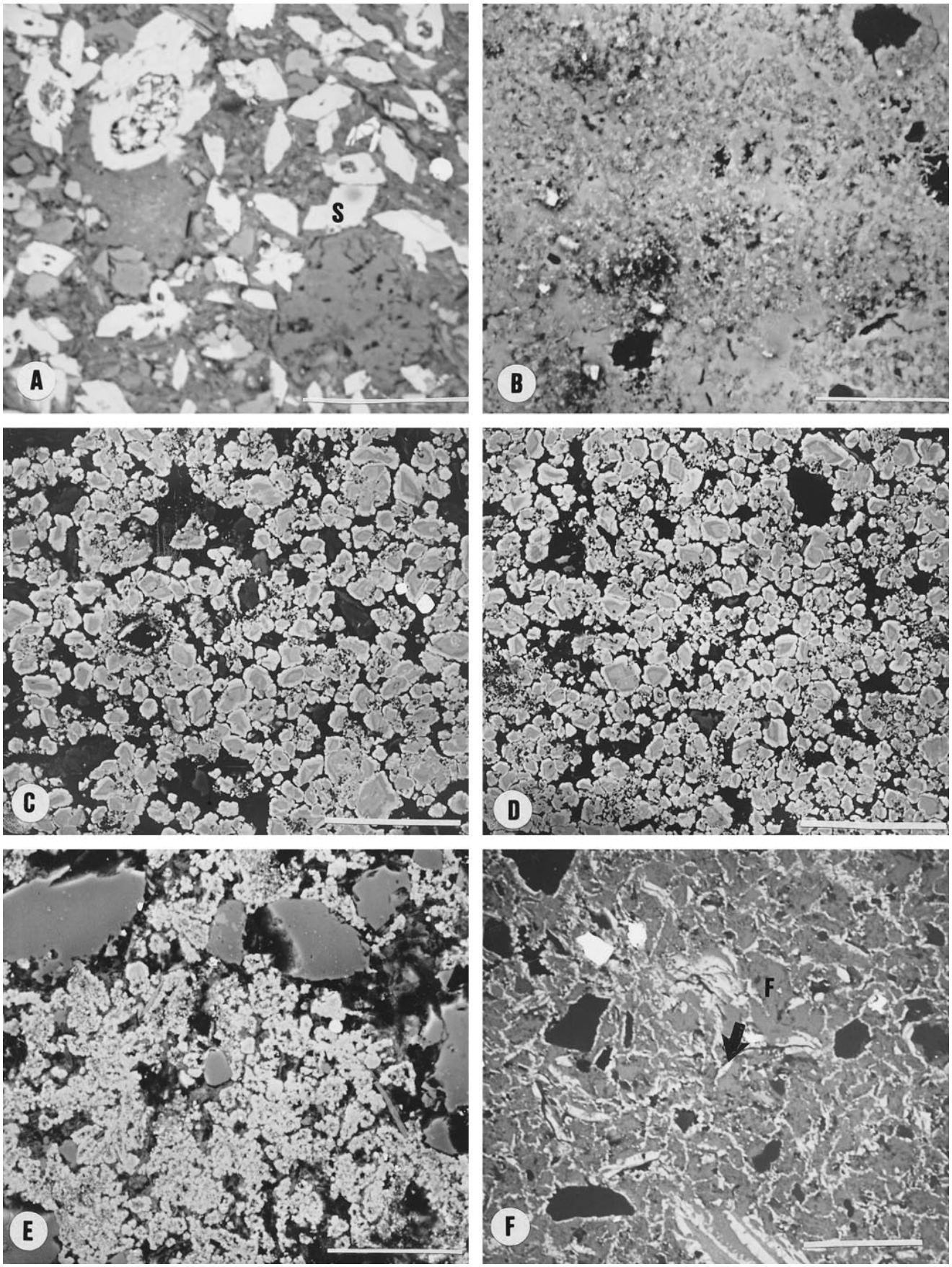
S
A
B
C
D
E
F
F

TABLE 1.—*Mean weight % oxide EDS analyses of siderite cements.*

Formation	Sample	Sedimentary Facies	Siderite Type	% Glauc. In Bed	FeO	MnO	CaO	MgO
Harwich	WH1	marine transressive	1	10 to 15	0.79	0.02	0.10	0.09
London Clay, A3	WH18A	shallow marine	2c	<1	0.79	0.01	0.10	0.10
London Clay, A3	WH18B	shallow marine	2c	<1	0.78	0.01	0.08	0.13
London Clay, top A3	WH8	shallow marine	3	≤5	0.81	<0.01	0.06	0.14
London Clay, B2	WH12A	shallow marine	2b (core)	absent	0.81	0.01	0.08	0.10
	WH12A		2b (rim)	absent	0.92	0.02	0.03	0.03
London Clay, B2	WH19	shallow marine	2c	trace	0.78	0.01	0.10	0.11
London Clay, D2	LCF5	lagoonal over shelf	2a (core)	1	0.83	0.02	0.08	0.07
			2a (rim)	1	0.91	0.04	0.03	0.02
London Clay, E	LCF6	lagoonal over shelf	2a	1	0.91	0.04	0.03	0.02
Wittering	WIT7	reworked	2a	5	0.91	0.04	0.03	0.02
Wittering	WIT9	intertidal over shelf	2a	10	0.83	0.04	0.07	0.06
Wittering	WIT13	lagoonal over shelf	2a	10	0.83	0.12	0.04	0.01
Wittering	WIT15	lagoonal over shelf	2a (core)	10	0.84	0.10	0.04	0.02
Wittering			2a (rim)	10	0.86	0.07	0.04	0.03
Wittering	WIT33	lagoonal	2a	2	0.88	0.06	0.05	0.01

Each data point is based on 5–10 days analyses. See text for details of sedimentary facies.

accurate; however, they fall within the overall range found at Whitecliff Bay. $\delta^{13}C$ values for the two samples analyzed are −14.29 and −12.93 VPDB, and those for $\delta^{18}O$ are −3.83 and −3.13 VPDB (Table 2).

DISCUSSION

Beneath oxygenated bottom waters, oxygen is rapidly removed by reaction with organic matter through the respiratory action of macroscopic or microscopic organisms. Beneath this oxic zone, whether in the sediment or the water column, Fe(III) is a major oxidant of organic matter, releasing Fe^{2+} to the pore water concomitantly (Froelich et al. 1979). Fe(III) reduction begins near the lower limit of the suboxic zone and continues until the Fe(III) supply is exhausted, which is commonly in the zone of methanogenesis. Beneath the oxic zone and immediately following the onset of Fe(III) reduction, sulfate-reducing bacteria utilize organic matter as a substrate, releasing both CO_2 and H_2S. The H_2S rapidly reacts with Fe^{2+} to produce iron sulfides. Where sulfate is lacking, as in freshwater environments, or after all sulfate has been utilized, methanogenic bacteria utilize organic matter, producing CO_2 and CH_4 (Claypool and Kaplan 1974). In the absence of H_2S, the concentration of Fe^{2+} in the porewater can increase. CH_4 production tends to raise the pH and, in the presence of appreciable aqueous Fe^{2+}, favors siderite precipitation (Claypool and Kaplan 1974; Berner 1981). It is evident from the above that siderite cement may form in any situation where sulfate is initially absent or removed, and where Fe and organic matter are sufficiently plentiful. This may be in a nonmarine sediment, in the diagenetic zone of pre—or post–sulfate reduction in marine sediments, in marine sediments penetrated by a freshwater wedge, or in marine sediments overlain by nonmarine sediments.

The bioturbated nature of the sediment in which the Whitecliff Bay siderite occurs suggests that sedimentation occurred in an oxic environment, whereas the association with glaucony identified as being *in situ* (Huggett and Gale 1997) with, or immediately above, all types of siderite (except 2b) indicates slow rates of deposition and relatively weak oxidizing conditions of formation. The restriction of Type 2a siderite concretions to sediments immediately beneath stratigraphic breaks (sequence boundaries) may reflect the time necessary for concretion growth.

Pyrite is present in all samples, although visual estimates suggest that the pyrite-to-siderite ratio is extremely low in Type 2a siderite. The lack of pyrite (typically < 1%) in association with Type 2a siderite suggests that sulfate reduction was inhibited through dilution of marine water by freshwater from overlying lagoonal or estuarine sediments. The slightly higher concentrations of pyrite (1–3%) associated with Types 1, 2b, and 2c siderite may reflect fully marine deposition. Subsequent penetration of a freshwater wedge into the shallow part of the basin may have diluted the marine pore waters, resulting in pore fluids ultimately more favorable to siderite precipitation. Alternatively, the siderite in marine sediments may predate or postdate sulfate reduction, although unless sedimentation is extremely slow it is unlikely that significant amounts could be precipitated in this way because sulfate reduction commences soon after burial. In the 2c concretions, where siderite rims are overgrown by pyrite and then ferroan calcite, the siderite is evidently pre–sulfate reduction. These possible scenarios are discussed below with the interpretation of the stable-isotope data.

The oxygen isotope composition of a mineral depends upon both the temperature and the isotopic composition of the water from which the minerals precipitated and the extent of any diagenetic resetting of the oxygen isotope composition, assuming that equilibrium relationships control $\delta^{18}O$. Freshwater is depleted in ^{18}O relative to seawater (values may be as low as −55‰ $\delta^{18}O$ SMOW), with the greatest depletion occurring at high altitudes and high latitudes (Longstaffe 1989). The oxygen isotope composition of siderite can be used to calculate a precipitation temperature if the composition of the precipitating water is assumed, or the composition of the water can be calculated if the temperature is known or assumed. The outcome of these calculations ultimately depends upon the fractionation equation used. The inorganic fractionation equation of Carothers et al. (1988) has been widely adopted. Recently, however, Mortimer and Coleman (1997) presented empirical data for microbial siderite and calculated fractionation equations for pure siderite, Mn-rich siderite, and Mg/Ca siderite. Precipitation temperatures calculated using the equation for microbial Mg/Ca siderite are compared with those obtained via the more widely used Carothers et al. (1988) equation (Table 2). The equations are:

Microbial Mg/Ca siderite $\quad 1000 \ln \alpha = 3.53 \times 10^6 T^{-2} - 12.4$ (Mortimer and Coleman 1997)

Inorganic siderite $\quad 1000 \ln \alpha = 3.13 \times 10^6 T^{-2} - 3.5$ (Carothers et al. 1988).

All the temperature calculations in Table 2 assume precipitation from seawater with a $\delta^{18}O$ SMOW of −1.2‰ (Shackleton and Kennett 1975). The justification for this assumption is discussed below. The Carothers et al. (1988) equation results in higher calculated temperatures than the Mortimer and Coleman (1987) relationship. Given that the latter describes microbial processes similar to or the same as those that result in early diagenetic siderite it is probable that they are more appropriate to the Whitecliff Bay siderite. If the temperatures calculated assuming precipitation from seawater are too high for the inferred diagenetic setting, meteoric-water mixing has in the past been invoked to reduce the calculated temperature, even when this contradicts sedimentological data (Machemer and Hutcheon 1988; Thyne and Gwinn 1994).

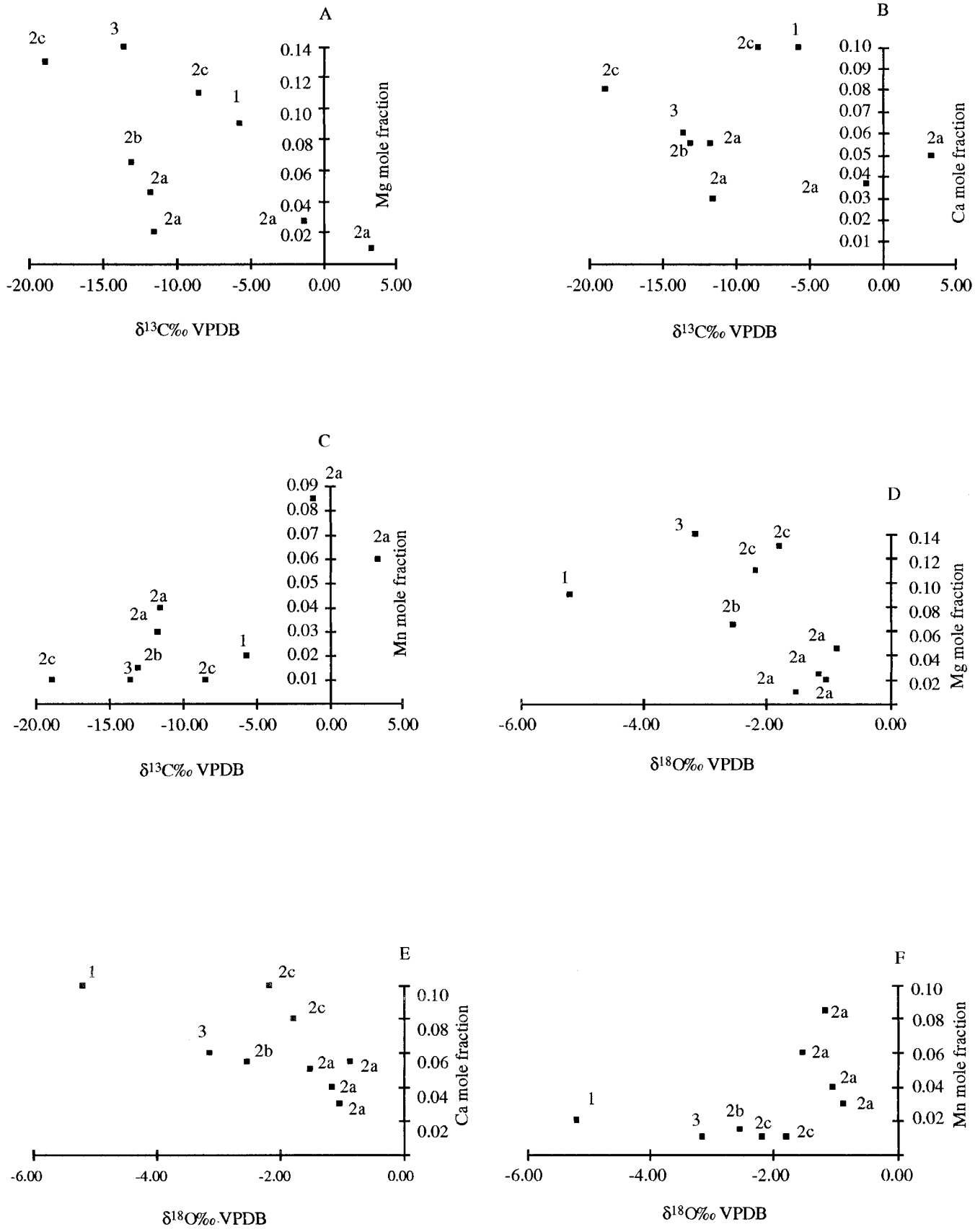

FIG. 5.—% MnO, CaO, and MgO plotted against ‰ $\delta^{13}C$ VPDB (A–C) and ‰ $\delta^{18}O$ VPDB (D–F). Mean values for both the oxides and the stable isotopes are used for each sample. Points are labeled to indicate the siderite type.

TABLE 2.—*Stable-isotope analyses and calculated temperatures, assuming precipitation from unmodified seawater with* $\delta^{18}O = -1.2$.

	Siderite Type	$\delta^{13}C$ PDB	$\delta^{18}O$ PDB	$\delta^{18}O$ SMOW	t°C (M & C)	t°C (Car)
WH1	1	−5.65	−5.50	25.20	28.6	50.5
WH8	3	−14.29	−3.83	26.92	22.0	41.6
WH8	3	−12.93	−3.13	27.63	19.6	38.0
WH12A	2b	−13.31	−2.62	28.16	17.7	35.6
WH12A	2b	−12.9	−3.13	27.63	19.6	38.0
WH18acalc	2c	−13.73	−6.63	24.03	33.0	57.0
WH18asid	2c	−11.82	−5.22	25.48	27.0	49.0
WH18bcalc	2c	−18.85	−4.71	26.01	25.5	46.0
WH18bsid	2c	−19.55	−2.13	28.66	16.0	33.0
WH19calc	2c	−5.57	−3.14	27.62	20.0	38.0
WH19sid	2c	−8.15	−2.52	28.27	17.0	35.0
LCF1/1	2a	−13.97	−1.06	29.78	12.0	28.3
LCF1/2	2a	−13.82	−0.42	30.43	10.0	25.0
LCF4/1	2a	−12.7	−0.92	29.92	11.8	27.6
LCF4/2	2a	−12.71	−0.81	30.03	11.4	27.0
LCF5/1	2a	−12.29	−1.39	29.43	13.4	29.8
LCF5/2	2a	−12.04	−1.18	29.64	12.7	28.8
LCF5/	2a	−10.77	−1.04	29.80	12.2	28.0
WIT7/1	2a(reworked)	−11.45	−0.87	29.97	11.6	27.0
WIT7/2	2a(reworked)	−11.77	−0.70	30.14	11.0	26.7
WIT7A	2a(reworked)	−11.5	−2.07	28.73	15.8	33.0
WIT7A	2a(reworked)	−11.46	−1.84	28.97	15.0	31.8
WIT15/1	2a	−2.12	−1.84	28.97	15.0	31.8
WIT15/2	2a	0.15	−1.30	29.52	13.0	29.4
WIT15	2a	−1.81	−1.49	29.33	13.7	30.3
WIT15	2a	1.39	−1.42	29.40	13.0	30.0
WIT33	2a	3.35	−2.09	28.70	15.8	33.0
WIT33	2a	3.31	−2.10	28.69	15.9	33.0
WIT33/1	2a	3.62	−1.81	29.00	15.0	31.7
WIT33/2	2a	3.55	−1.72	29.09	14.5	31.3
WIT33/4	2a	3.57	−1.77	29.04	15.0	31.6
WIT33/5	2a	3.99	−1.79	29.02	15.0	31.7
WIT33/6	2a	3.97	−1.72	29.09	14.5	31.3

(M C) indicates that the equation of Mortimer and Coleman (1997) for Mg/Ca microbial siderite was used, (Car) indicates that the equation of Carothers et al. (1988) for inorganic siderite was used.

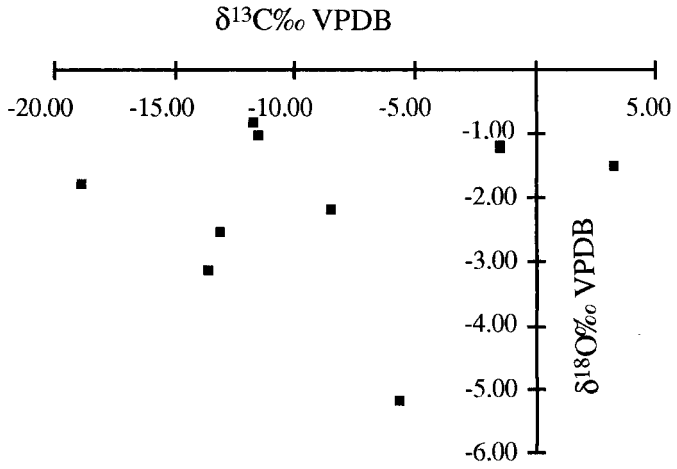

FIG. 6.—Values of ‰ $\delta^{13}C$ VPDB plotted against values of ‰ $\delta^{18}O$ VPDB (all data).

Sulfate reduction with concomitant oxidation of organic matter typically results in dissolved CO_2 with $\delta^{13}C$ values of −25 to −28‰ (Presley and Kaplan 1968). CO_2 derived through fermentation of organic matter may result in either negative or positive $\delta^{13}C$ values, depending on the precise reaction involved (Whiticar et al. 1986; Fisher et al., 1998). However, in the diagenetic environment fermentation generally results in CH_4 with a $\delta^{13}C$ of approximately −75‰ (Claypool et al. 1973), from which Irwin et al. (1977) estimate that the CO_2 has a $\delta^{13}C$ value of +15‰. The $\delta^{13}C$ values we obtained range from −19.55‰ to +3.99‰, which is typical for marine siderites (Mozley and Burns 1993). This range of $\delta^{13}C$ values suggests that the carbonate was a product of bacterial reduction of iron and sulfate, with minor methanogenic fermentation and possibly marine carbonate dissolution (which has a $\delta^{13}C$ value close to zero). The latter is most likely to be present in the Type 2a concretions with articulated crustaceans, because the latter indicate extremely early cementation. No inverse correlation is apparent between $\delta^{18}O$ and $\delta^{13}C$ (Fig. 6), which may indicate that the proportion of methanogenic carbonate did not increase steadily with increasing temperature (decreasing $\delta^{18}O$) or depth of burial. If the $\delta^{18}O$ values are controlled by freshwater influx, however, a negative correlation with $\delta^{13}C$ would not be expected.

The influence of environment on carbonate composition is evident from comparison of previously published data for impure marine siderite (Mozley 1989; Jordan et al. 1992) with data for nonmarine, pure siderite with occasional Mn concentric banding (Gibson et al. 1994). Mozley (1989) suggested that low Fe/(Ca + Mg) in earliest formed siderite reflects the low Fe/(Ca + Mg) of the relatively unaltered suboxic marine water from which it precipitated. Jordan et al. (1992), however, reported an increase in Ca and a decrease in Mn from core to margin, with an almost constant proportion of Fe. These differences in chemical trends between fully marine siderites described by Mozley (1989) and Jordan et al. (1992) suggest that other factors, such as temperature or timing relative to other diagenetic reactions, may also be important.

In the Whitecliff Bay siderites, substitution for Fe by Ca and Mg increases, and substitution by Mn decreases, with decreasing bulk $\delta^{18}O$ (Fig. 6D–F). If decreasing $\delta^{18}O$ is interpreted as indicating increasing temperature, this chemical trend is consistent with the findings of McKay et al. (1995) and Curtis et al. (1975), both of whom found a decrease in Mn and Fe with time of precipitation. The converse trend (i.e., increase in Fe and Mn with decrease in Ca and Mg; see Table 1) from core to margin in zoned cement may also reflect a fundamental change in depositional environment of the overlying sediment. Type 2a concretions formed in fully marine sediments beneath long-lived submarine erosion surfaces; lowstand deposits are entirely missing, and subsequent estuarine progradation introduced brackish pore fluid. The more Fe- and Mn-rich siderite may have precipitated during this brackish influx; however, the $\delta^{18}O$ values (for the combined cement zones) are some of the highest in this data set (Table 2). This apparent discrepancy is discussed below.

To calculate the oxygen isotope composition of the water from which the siderite precipitated (i.e., whether it was fresh or marine) it is necessary to know the temperature of precipitation. Purton (1997) provided a paleotemperature of 24–25°C derived from $\delta^{18}O$ data for *Nummulites prestwichianus* from the base of the Barton Group (immediately above the Bracklesham Group); Andreasson and Schmitz (1996) determined a mean annual range of 14–28°C from $\delta^{18}O$ data from Lutetian gastropods (equivalent to the Bracklesham Group) of the French part of the same basin; and Buchardt (1978) calculated (from foraminifera $\delta^{18}O$ data) an Ypresian (Early Eocene) temperature range of 20–28°C for the North Sea. All these temperatures are for bottom water. Assuming precipitation from seawater $\delta^{18}O$ value of −1.2‰, most of the temperatures calculated using the Mortimer and Coleman (1997) equation are within this range (Table 1); however, temperatures for siderite Types 2a and 2b are slightly low (Table 2). Using the Carothers et al. (1988), equation, only siderite Types 2a and 2b have calculated precipitation temperatures compatible with the fossil-carbonate-derived temperatures. As Mortimer and Coleman (1997) demonstrated, with Mn mole fractions of up to 0.13 (WIT13), a different fractionation equation would be more appropriate. The conventional argument to explain higher than expected temperatures is to invoke mixing of seawater with meteoric water (which has a variable $\delta^{18}O$ value but one that is always more negative than seawater). This is entirely consistent with the scenario suggested above whereby the composition of concretions in marine sediments is influenced by subsequent estuarine progradation. However, if we accept that the Mortimer and Coleman (1997) equation for microbial Mg/Ca siderite

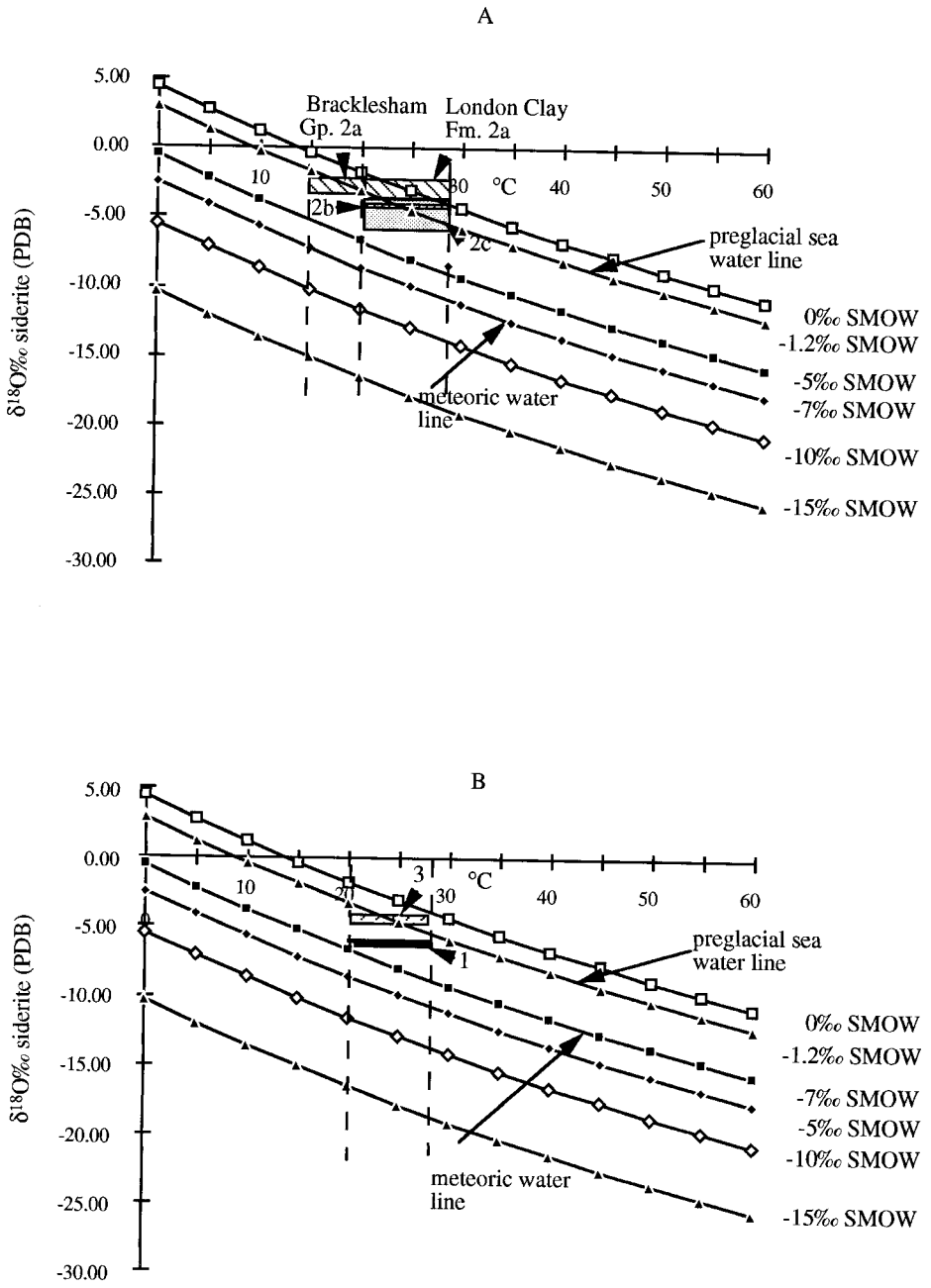

FIG. 7.—Values of ‰ δ^{18}O VPDB for siderites plotted against precipitation temperature, with the calculated isotopic compositions of the fluids from which they may have formed, assuming isotopic equilibrium. The water lines were calculated using the fractionation equation of Mortimer and Coleman (1997) for microbial Mg/Ca siderite. **A)** Type 1 and Type 3 siderite, formation temperature range of 14–28°C assumed; **B)** Types 2a, 2b, and 2c siderite, formation temperature range of 20–28°C assumed.

is the most appropriate, then meteoric input would depress the calculated temperatures still further. Type 2c siderite is associated only with marine sediment overlain by marine sediment and is probably earlier than most of the other siderite types, being pre–sulfate reduction. Type 2c siderite δ^{18}O values are consistently higher than those of the associated calcite, which is consistent with both being marine cements.

If the extent of water mixing were the only factor controlling siderite isotopic composition, the temperature calculated presuming precipitation from seawater would be expected to increase from fully marine facies (Types 1, 2b, 2c, and 3 siderite) to marine overlain by lagoonal and estuarine facies (Type 2a siderite), which is not the case (Table 2). Type 2a siderite actually has the highest δ^{18}O values, yet it is invariably overlain by lagoonal sediment. This suggests that it is not the brackish influx which is important to concretion formation but rather the break in sedimentation.

The Type 2a siderite occurs only in glauconitic sediments at the very top of the London Clay Formation and in the Bracklesham Group, for which mean bottom water temperatures may have been as low as 14°C. The Type 2a siderite δ^{18}O values may simply reflect climatic cooling towards the top of the London Clay Formation. For Type 2a siderite to precipitate without the influence of freshwater requires that it either predates sulfate reduction or the carbonate is post–sulfate reduction (i.e., methanogenesis, which would give positive δ^{13}C values, e.g. WIT33). Precipitation of both glaucony and pre–sulfate reduction siderite require sufficient concentrations of organic matter and Fe, plus a long residence time in the suboxic zone. All the Type 2a siderites are associated with glaucony beneath long-lived erosional surfaces, allowing formation of pre–sulfate reduction siderite. Faunal evidence and estimated water depths (Huggett and Gale 1997, 1998) suggest that it is unlikely that freshwater dilution occurred beneath these erosion surfaces. The requirements for glaucony and pre–sulfate reduction siderite are therefore met. WIT33 is from the

interval with least marine influence (Huggett and Gale 1997), where sulfate reduction might be expected to give way to methanogenesis sooner than where marine influence was stronger. Organic matter and iron not utilized in the suboxic zone for formation of glaucony and siderite would therefore be available in the zone of methanogenesis. This might explain why WIT33 has heavier carbon isotope values than other concretions. WIT15 has $\delta^{13}C$ values intermediate between the London Clay Formation concretions and WIT33. This suggests that WIT15 has a combination of pre–sulfate reduction and methanogenic siderite.

If the mean temperature of bottom water and sediment is assumed to be 20–28°C for the London Clay Formation and 14–28°C for the Bracklesham Group, and the siderite is assumed to precipitate in isotopic equilibrium with the precipitating water, the composition of the water and hence the degree of meteoric input can be calculated (Fig. 7). The water-composition lines in Figure 7 were calculated using the fractionation equation of Mortimer and Coleman (1997) for microbial Mg/Ca siderite. Seawater is the −1.2‰ SMOW line; the meteoric-water composition is not known, but it is presumed to be more negative than seawater. These calculated data show that the formation fluids had a mixed marine/meteoric composition for Type 1 siderite (Fig. 7A), which is compatible with a very shallow marine environment of formation where a freshwater wedge may have been present. For Types 2b and 3, both of which formed in marine sediment with no subsequent meteoric overprint, the inferred fluid is also marine. For the Type 2c siderites, with WH18a and WH18b being from a shallow marine interval and WH19 from marine sediment 4 m below a lagoonal interval, calculated water compositions are consistent with the inferred marine water with some meteoric input. Textural relationships and temperatures calculated from $\delta^{18}O$ values indicate that siderite in the Type 2c concretions predates calcite, which suggests that it precipitated pre–sulfate reduction. Bracklesham Group Type 2a siderite concretions are also from marine sediment beneath nonmarine sediment; however, because a higher temperature is assumed for the Type 2a siderite of the London Clay Formation, the calculated formation fluids would have a fully marine composition. In this instance, for the siderite to have a fully marine signature (if the temperature estimates are correct) requires no subsequent invasion by brackish water from overlying sediments, or the concretions formed prior to deposition of the nonmarine sediments or the brackish water had little impact upon the siderite. This suggests that the Type 2a siderite of the London Clay Formation is indeed pre–sulfate reduction.

SUMMARY

(1) Siderite cements in the Eocene of Whitecliff Bay occur in a range of sedimentary facies and with a range of morphological relationships. The association between glaucony and siderite (Types 1 and 2a siderite) illustrates the importance of slow deposition for precipitation of concretionary carbonate. Type 2a siderite concretions occur only beneath breaks in deposition where meteoric water may have been introduced, though the time involved in the break may be a more important factor in concretion formation than the introduction of meteoric water for these examples. Siderite cement may be formed in any situation where sulfate is scarce or absent. This may be in a nonmarine sediment, in the diagenetic zone of pre—or post–sulfate reduction in marine sediments, in marine sediments penetrated by a freshwater wedge, or in marine sediments overlain by nonmarine sediments with associated penetration of meteoric fluids.

(2) Siderite cements in the Eocene sediments of Whitecliff Bay are without exception impure, and most are zoned. The degree of total mole substitution for Fe decreases from around 10% in the core to 5% at the rim in zoned cement crystals. Trends for individual cations (Ca, Mg, and Mn) vary, but where Ca and Mg decrease from core to rim, Mn increases and vice versa. Marine siderite generally has a lower (Fe + Mn)/(Ca + Mg) ratio than nonmarine siderite. This may be the cause of siderite chemical zonation (at the scale of individual crystals) where estuarine sediments overlie marine sediments with siderite concretions (Type 2a siderite).

(3) Whole-rock stable-isotope data for zoned siderites might be expected to reflect the relative proportions of the chemical zones. However, the seemingly similarly zoned LCF5 and WIT15 (mostly early Fe-poor siderite; Fig. 4C–D) have quite different carbon isotope values. WH12a, which is dominated by the late Mn/Fe-rich siderite (Fig. 4E) has $\delta^{18}O$ and $\delta^{13}C$ isotopic values similar to those of LCF5.

(4) The differences among the precipitation temperatures calculated using the Mortimer and Coleman (1997) equation for microbial siderite and the Carothers et al. (1988) equation for inorganic siderite illustrate the importance of using the correct fractionation equation. Regardless of the equation used, however, not all the calculated precipitation temperatures fall within with expected temperature ranges based on independent temperature evidence and estimates of seawater $\delta^{18}O$. Further refinement of the fractionation equations may allow better temperature estimates to be made in future.

(5) Precipitation temperatures calculated using the Mortimer and Coleman (1997) equation for microbial Mg/Ca siderite, and based on the assumption that precipitation occurred from seawater, are reasonable for siderite Types 1 and some 2c and 3. For Types 2a, 2b and some 2c, however, calculated precipitation temperatures are low relative to temperature ranges estimated from $\delta^{18}O$ of marine bioclasts (Buchardt 1978; Andreasson and Schmitz 1996; Purton 1997). Meteoric input would make these calculated temperatures lower still; therefore we propose that meteoric input was not a major factor in these examples. If the equation of Carothers et al. (1988) for inorganic siderite is used, the majority of the calculated temperatures are too high but may be lowered to match the bioclast temperature range if a meteoric component is assumed.

(6) If a range of precipitation temperatures is assumed, and the siderite is assumed to have precipitated in isotopic equilibrium with the precipitating water, the composition of the water, and hence the degree of meteoric input, can be calculated. The results are generally compatible with the inferred depositional environments. For the London Clay Formation, it is not necessary to invoke input from overlying lagoonal sediments for precipitation of Type 2a siderite, but for some Type 2c siderites freshwater input is necessary.

(7) It is clear from the above that for stable isotopes to be of unequivocal value in understanding the diagenetic environment in which siderite precipitates, other factors must be constrained. For example, precipitation temperatures and the hydrological regime must be understood. The interpretation could also be improved if siderite chemical zones from individual crystals were separated for stable-isotope analysis.

ACKNOWLEDGMENTS

Samples for BSEM were prepared by Liz Morris, and XRD analyses were carried out by Martin Gill, both of Imperial College. Walter Dean, Tim Lyons, and Rob Raiswell are thanked for their helpful reviews.

REFERENCES

Al-Aasm, I.S., Taylor, B.E., and South, B., 1990, Stable isotope analysis of multiple carbonate samples using selective acid extraction: Chemical Geology, v. 80, p. 119–125.

Al-Agha, M.R., Burley, S.D., Curtis, C.D., and Esson, J., 1995, Complex cementation textures and authigenic mineral assemblages in Recent concretions from the Lincolnshire Wash (east coast, UK) driven by Fe(0) to Fe(II) oxidation: Geological Society of London, Journal, v. 152, p. 157–171.

Andreasson, F.P., and Schmitz, B., 1996, Winter and summer temperatures of the early middle Eocene of France from *Turritella* $\delta^{18}O$ profiles: Geology, v. 24, p. 1067–1070.

Berner, R.A., 1981, A new geochemical classification of sedimentary environments: Journal of Sedimentary Petrology, v. 51, p. 359–365.

Buchardt, B., 1978, Oxygen isotope palaeotemperatures from the Tertiary period in the North Sea area: Nature, v. 275, p. 121–123.

Carothers, W.W., Adami, L.H., and Rosenbauer, R.J., 1988, Experimental oxygen isotope fractionation between siderite–water and phosphoric acid liberated CO_2–siderite: Geochimica et Cosmochimica Acta, v. 52, p. 2445–2450.

CLAYPOOL, G.E., AND KAPLAN, I.R., 1974, The origin and distribution of methane in marine sediments, *in* Kaplan, I.R., ed., Natural Gases in Marine Sediments: New York, Plenum Press, p. 99–139.

CLAYPOOL, G.E., PRESLEY, B.J., AND KAPLAN, I.R., 1973, Gas analyses in sediment samples from Legs 10, 11, 13, 14, 15, 18 and 19, *in* Creager, J.S. and Scholl, D.W., eds., Initial Reports of the Deep Sea Drilling Project, v. 19, Part 1: Washington, D.C., U.S. Government Printing Office, p. 879–894.

CURTIS, C.D., PEARSON, M.J., AND SOMOGYI, V.A., 1975, Mineralogy, chemistry and origin of a concretionary siderite sheet (clay-ironstone band) in the Westphalian of Yorkshire: Mineralogical Magazine, v. 40, p. 385–393.

FISHER, Q.J., RAISWELL, R., AND MARSHALL, J.D., 1998, Siderite concretions from non-marine shales (Westphalian A) of the Pennines, England: controls on their growth and composition: Journal of Sedimentary Petrology, v. 68, p. 1034–1045.

FROELICH, P.N., KLINKHAMMER, G.P., BENDER, M.L., LUEDTKE, N.A., HEATH, G.R., DAUPHIN, P., HAMMOND, D., HARTMAN, B., AND MAYNARD, V., 1979, Early oxidation of organic matter in pelagic sediments of the eastern equatorial Atlantic: sub-oxic diagenesis: Geochimica et Cosmochimica Acta, v. 43, p. 1075–1090.

GIBSON, P.J. SHAW, H.F., AND SPIRO, B., 1994, The nature and origin of sideritic ironstone bands in the Tertiary Lowmead and Duaringa Basins, Queensland: Australian Journal of Earth Sciences, v. 41, p. 255–263.

HUGGETT, J.M., AND GALE, A.S., 1997, Petrology and palaeoenvironmental significance of glauconiy in the Eocene Succession at Whitecliff Bay, Hampshire Basin, U.K.: Geological Society of London, Journal, v. 154, p. 897–912.

HUGGETT, J.M., AND GALE, A.S., 1998, Petrography and diagenesis of the Thames Group at Whitecliff Bay, Isle of Wight, U.K.: Proceedings of the Geologists' Association, v. 109, p. 99–113.

IRWIN, H., CURTIS, C.D., AND COLEMAN, M., 1977, Isotopic evidence for source of diagenetic carbonates formed during burial of organic-rich sediments: Nature, v. 269, p. 209–213.

JORDAN, M.M., CURTIS, C.D., APLIN, A.C., AND COLEMAN, M.L., 1992, Access of pore waters to carbonate precipitation sites during concretion growth (extended abstract), *in* Kharaka, Y.K., and Maest, A.S. eds., 7th International Symposium on Water–Rock Interactions, Utah, U.S.A., Proceedings: Rotterdam, Balkema, p. 1239–1242.

KING, C., 1981, The Stratigraphy of the London Clay and Associated Deposits: Rotterdam, Backhuys, 158 p.

LONGSTAFFE, F., 1989, Stable isotopes as tracers in clastic diagenesis, *in* Hutcheon, I.E., ed., Short Course in Burial Diagenesis: Toronto, Mineralogical Association of Canada, p. 201–257.

MACHEMER, S.D., AND HUTCHEON, I., 1988, Geochemistry of early carbonate cements in the Cardium Formation, central Alberta: Journal of Sedimentary Petrology, v. 58, p. 136–147.

MCKAY, J.L., LONGSTAFFE, F.J., AND PLINT, A.G., 1995, Early diagenesis and its relationship to depositional environment and relative sea-level fluctuations (Upper Cretaceous Marshybank Formation, Alberta and British Columbia): Sedimentology, v. 42, p. 161–190.

MATSUMOTO, R., 1989, Isotopically heavy oxygen-containing siderite derived from the decomposition of methane hydrate: Geology, v. 17, p. 707–710.

MORTIMER, R.J.G., AND COLEMAN, M.L., 1997, Microbial influence on the oxygen isotopic composition of diagenetic siderite: Geochimica et Cosmochimica Acta, v. 61, p. 1705–1711.

MOZLEY, P.S., 1989, Relation between depositional environment and the elemental composition of early diagenetic siderite: Geology, v. 17, p. 704–706.

MOZLEY, P.S., AND BURNS, S.J., 1993, Oxygen and carbon isotopic composition of marine carbonate concretions: an overview: Journal of Sedimentary Petrology, v. 63, p. 73–83.

MOZLEY, P.S., AND CAROTHERS, W.W., 1992, Elemental and isotopic composition of siderite in the Kuparak Formation, Alaska: effect of microbial activity and water/sediment interaction on early pore-water chemistry: Journal of Sedimentary Petrology, v. 62, p. 681–692.

MOZLEY, P.S., AND HOERNLE, K., 1990, Geochemistry of carbonate cements in the Sag River and Shublik Formations (Triassic/Jurassic), North Slope, Alaska: implications for the geochemical evolution of formation waters: Sedimentology, v. 37, p. 817–836.

PEARSON, M.J., 1974, Siderite concretions from the Westphalian of Yorkshire: a chemical investigation of the carbonate phase: Mineralogical Magazine, v. 39, p. 696–699.

PLINT, A.G., 1983, Facies, environments and sedimentary cycles in the Middle Eocene, Bracklesham Formation of the Hampshire Basin: evidence for global sea-level changes?: Sedimentology, v. 30, p. 625–653.

PLINT, A.G., 1988, Global eustacy and the Eocene sequence in the Hampshire Basin England: Basin Research, v. 1, p. 11–22.

PRESLEY, B.J., AND KAPLAN, I.R., 1968, Changes in dissolved sulphate, calcium and carbonate from interstitial water of near shore sediments: Geochimica et Cosmochimica Acta, v. 32, p. 1037–1048.

PURTON, L.M.A., 1997, Geochemical approaches to the problem of nummulitic life habit and habitat in the Eocene [unpublished D.Phil. thesis]: Oxford University, 214 p.

PYE, K., DICKSON, J.A.D., SCHIAVON, N., COLEMAN, M.L., AND COX, M., 1990, Formation of siderite–Mg-calcite–iron sulphide concretions in intertidal marsh and sandflat sediments, north Norfolk, England: Sedimentology, v. 37, p. 325–343.

ROSENBAUM, J., AND SHEPPARD, S.M.F., 1986, An isotopic study of siderites, dolomites and ankerites at high temperatures: Geochimica et Cosmochimica Acta, v. 50, p. 1147–1150.

SHACKLETON, N., AND KENNETT, J.P., 1975, Late Cenozoic oxygen and carbon isotopic changes at DSDP site 284: implications for glacial history of the Northern Hemisphere, *in* Kennett, J.P., Houtz, R.E., et al., eds., Initial Reports of the Deep Sea Drilling Project, v. 29: Washington, D.C., U.S. Government Printing Office, p. 801–807.

THYNE, G.D., AND GWINN, C.J., 1994, Evidence for a paleoaquifer from early diagenetic siderite of the Cardium Formation, Alberta, Canada: Journal of Sedimentary Petrology, v. 64, p. 726–732.

WHITICAR, M.J., FABER, E., AND SCHOELL, M., 1986, Biogenic methane formation in marine and freshwater environments: CO_2 reduction vs. acetate fermentation—Isotopic evidence: Geochimica et Cosmochimica Acta, v. 50, p. 693–709.

Received 7 November 1997; accepted 23 November 1999.